Image-based versus atlas-based patient-specific S-value assessment for Samarium-153 EDTMP cancer palliative care: A short study

Original Article

Maryam Fallahpoor[1], Mehrshad Abbasi[1], Ali Asghar Parach[2], Ahmad Bitarafan Rajabi[3,4], Faraz Kalantari[5]

[1]Department of Nuclear Medicine, Vali-Asr Hospital, Tehran University of Medical Sciences, Tehran, Iran
[2]Department of Medical Physics, Shahid Sadoughi University of Medical Sciences, Yazd, Iran
[3]Echocardiography Research Center, Cardiovascular Interventional Research Center, Rajaie Cardiovascular Medical and Research Center, Iran University of Medical Sciences, Tehran, Iran
[4]Department of Nuclear Medicine, Rajaie Cardiovascular Medical and Research Center, Iran University of Medical Sciences, Tehran, Iran
[5]Department of Radiation Oncology, UT Southwestern Medical Center, Dallas, Texas, USA

(Received 8 September 2017, Revised 16 December 2017, Accepted 22 December 2017)

ABSTRACT

Introduction: Use of SPECT/CT data is the most accurate method for patient-specific internal dosimetry when isotopes emit single gamma rays. The manual or semi-automatic segmentation of organs is a major obstacle that slows down and limits the patient-specific dosimetry. Using digital phantoms that mimic patient's anatomy can bypass the segmentation step and facilitate the dosimetry process. In this study, the results of a patient-specific dosimetry based on CT data and XCAT phantom, a flexible phantom with predefined organs, are compared.

Methods: The dosimetry results (S-value and SAF) were calculated for a patient with breast cancer who received Samarium-153 ethylenediamine-N,N,N′,N′-tetrakis(methylenephosphonic acid (^{153}Sm-EDTMP). Biodistribution of activity was obtained from the SPECT scan. The anatomical data and attenuation map were extracted from CT as well as the XCAT phantom with different BMIs. GATE Monte-Carlo simulator was used to calculate the dose to different organs based on the activity distribution and segmented anatomy.

Results: The whole body dosimetry results are the same for both calculations based on the CT and XCAT with different BMIs; however for target organs, the differences between SAFs and S-values are high. In the spine, the clinically important target organ for Samarium therapy, the dosimetry results obtained from phantoms with unmatched BMIs between XCAT phantom and CT are substantially different.

Conclusion: We showed that atlas-based dosimetry using XCAT phantom even with matched BMI may lead to considerable errors as compared to calculations based on patient's own CT. For accurate dosimetry results, calculations should be done using CT data.

Key words: ^{153}Sm-EDTMP; Dosimetry; XCAT phantom; Atlas-based dosimetry; Radio-targeted therapy

Iran J Nucl Med 2018;26(2):76-81
Published: July, 2018
http://irjnm.tums.ac.ir

Corresponding author: Dr Mehrshad Abbasi, Department of Nuclear Medicine, Vali-Asr Hospital, Tehran University of Medical Sciences, Tehran, Iran. E-mail: meabbasi@tums.ac.ir

INTRODUCTION

Image-based internal dosimetry has been a major area of research over recent years [1-4]. Patient-specific dosimetry is the most accurate method for systemic radiation treatment planning [5, 6]. Specific information is required including activity distribution and organ boundaries for patient-specific dosimetry. CT data provides anatomical information which can be used for defining volume of interests specifying internal organs. Hybrid SPECT/CT functional imaging allows the lesions visible in functional imaging modality to be correlated with anatomical structures [7]. For internal dosimetry purposes, SPECT/CT provides anatomical and functional imaging in a single session and has the important option for SPECT activity quantification and the data of both biodistribution of the activity and the anatomy of the organs being collected simultaneously [8]. Nevertheless, using CT images for segmentation of anatomic structures of patient body, despite being more accurate, is time consuming. The alternative is using phantoms or atlas data with already segmented organs and known organ boundaries. The anatomical structures are derived from these databases very easily. However, the variability of radiotracers' biodistribution and differences of anatomical structures are remarkable among patients which hinder accurate application. Newly developed sophisticated humanoid phantoms may fit more with the patient's specifications and overcome this obstacle. The 4D-extended cardiac-torso (XCAT) phantom [9] is a flexible phantom that can be used for different purposes. XCAT phantoms can be generated for both genders with different resolutions and voxel sizes and for different body mass indices (BMI). The critical concern which will be addressed in this paper is whether the results are similar to methods that use patient's CT. In this research, we address this concern through an experimental study. The CT data was obtained from a patient treated with Samarium-153 ethylenediamine-N,N,N′,N′-tetrakis(methylenephosphonic acid (^{153}Sm-EDTMP) for multiple bone metastases from breast cancer. ^{153}Sm-EDTMP is used for pain palliation therapy in end stage patients with intractable bone pain [10].

For dosimetry calculations GATE (GEANT4 Application to Tomographic Emission) [11], a Monte Carlo based script interface dedicated to nuclear medicine, was used. Different versions of this free open source toolkit are available on the openGATE collaboration website. It was primarily developed for simulation of imaging processes of PET, SPECT [11, 12] and CT [13, 14] and it is validated for internal dose calculations [15]. For dosimetry applications, GATE is capable to take either patient's CT or a digital atlas phantom as input [16]. GATE has certain attractive features; some of them are inherited from GEANT4 [17] and some are additionally developed. These include flexible simulation geometry capable of accommodating a large variety of detector and source details and the physical events. The software provides a user-friendly voxelized source, a virtual clock allowing to simulate temporal phenomena such as source and detector movements and source decay, and a large variety of physical models (i.e. photo-nuclear and photo-media reactions). Using GATE, we compared the specific absorbed fraction (SAF) and S-values (the mean absorbed dose to the target organ from unit activity of the relevant radioisotope distributed within the source organ/s) for gamma and beta emissions from ^{153}Samarium using a patient's CT and XCAT phantom with either matched or unmatched BMIs.

METHODS

Patient study

A 50 year old female –now passed away– with widespread bone metastases from breast cancer was slowly injected with 150 mCi activity of ^{153}Sm-EDTMP intravenously. The patient had a BMI of 38.3. Eighteen hours after the tracer injection, patient underwent SPECT/CT imaging. The Simens Simbia T SPECT/CT scanner was used for the imaging. SPECT/CT images between the chest and the abdomen were obtained. For SPECT imaging, 64 projections were acquired with 20 second per projection. The matrix size of SPECT was 64×64 with pixel size of 9.59 mm. The low dose CT component, with the arc of 360̊, 130 kVp and 30mA, was used. The CT image provided an attenuation map for attenuation correction and aided the localization of organs.

SPECT reconstruction was performed using iterative ordered-subsets expectation maximization algorithm (OSEM). The reconstruction used 8 iterations and 4 subsets, Gaussian diffusion resolution recovery and CT-based attenuation correction. For the SPECT image, all the available corrections was done including the main one, attenuation correction. We also performed calibration for Samarium. Absorbed dose estimation requires longitudinal studies and several imaging. Our study addresses the effect of anatomical differences on S-values which is a dosimetric parameter and related to the absorbed dose. SPECT and CT image fusion was performed with SPECT/CT fusion software automatically and with manual fine tuning afterwards.

The semi-automatic segmentation of the organs in the CT image was performed using itk-SNAP [18] (version 2.4.0) software. Eight organs that are important in Samarium therapy were segmented in addition to the body as a whole. Validations are performed by comparison between segmented organs and organs in patient' CT image visually. An ID was assigned to each organ which was used as input to GATE. We assigned each segmented organ ID the

corresponding material to be used for dosimetry using GATE [19].

XCAT phantom study

XCAT phantom is a CT based-hybrid phantom that have some capability to replicate some characteristics of the real patients but not all. We changed as many characteristic as possible in XCAT including selecting the most fitted BMI to produce the phantom that has the most similarity to our patient. The XCAT phantom was generated based on the patients characteristics (female with BMI= 38.8 and right side mastectomy) and CT specification (matrix size and voxel size). The following parameters were employed: 64×64 for matrix size, 60 for number of slices and 9.59 mm for voxel size (Figure 1). We also designed XCAT phantoms with BMIs of 36.7 and 35.5 and compared them with the results from patient BMI matched phantom. Different numbers were assigned to XCAT different organs so that every organ had a unique ID number. Corresponding μ values were mapped later from the GATE material data base.

Monte Carlo simulation

For both simulations of patient-specific dosimetry with the CT and XCAT phantom, the same SPECT image was used as the activity map. The simulations were performed in GATE Monte Carlo code (version 6.0.0). The data of SPECT, CT and XCAT phantoms were processed to prepare suitable input file formats for GATE. The results of the internal dosimetry for the real activity distribution in the patient body based on the SPECT data were calculated for the CT image and the XCAT phantom in the kidney, liver, heart, spleen, bladder, lung, ribs, and spine as well as in the total body. Photoelectric absorption, Compton and Reyleigh scattering, ionizations, multiple scattering and bremsstrahlung photons were simulated. After completion of simulations, GATE produced two binary files, containing respectively the absolute absorbed dose delivered into the voxels (in cGy) and the corresponding uncertainties [20]. The uncertainty is the relative statistical error and expressed as a fraction between 0 and 1.

Dosimetry calculations

The results of dosimetry calculations are presented according to Medical International Radiation Dose (MIRD) committee formalism [21]; specific absorbed fraction (SAF) was calculated as the fraction of energy emitted by the radioisotope in the source organ (r_s), that is absorbed in the target organ (r_t) per unit mass of the target organ (m_t).

$$SAF(r_t \leftarrow r_s) = \frac{r_t/r_s}{m_t}$$

The S-value has a unit of mGy/MBq-s. In theory, the relation is given by $S = \sum_i \Delta i \times SAF$, where Δi is the mean energy of the i^{th} transition per nuclear transformation of a specific isotope [22]. Since we are comparing results from monoenergetic particles, the relation reduces to S = E × SAF, where E is the energy of the ^{153}Samarium.

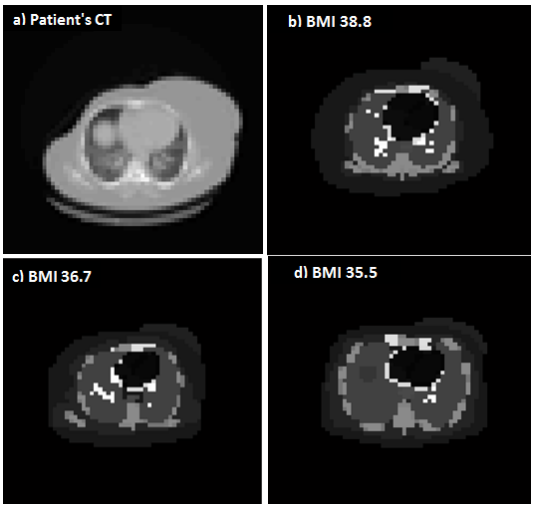

Fig 1. A typical transverse slice of CT image and XCAT phantom; a) Patient's CT, b) BMI 38.8, c) BMI 36.7 and d) BMI 35.5.

RESULTS

It is common that the results of the dosimetry are reported in SAF for gamma radiation and S-value for the beta emission. Given Samarium-153 has both decay mode, we reported SAF for 103 keV gamma radiation and S-value for 0.801 MeV beta emission. The SAFs for gamma and S-values for beta emissions are presented in Table 1. The organ of interest for this particular radiotracer is the spine. The S-value for the spine, is 1.83e-05 when patient CT is used and 0.84580e-5 when XCAT phantom with BMI=38.8 is employed, also the SAF for the spine is 0.0566 using CT data and 0.0414 using XCAT phantom. The difference in SAFs and S-value for the spine is 26.8% and 53.8% respectively. The highest differences in the S-values are observed for the ribs (70.7%) and bladder (-109%). The highest difference among the SAFs is for the liver (27.6%).

The results of two other different BMIs (i.e. 36.74 and 35.53) are presented in Table 2. For the XCAT phantom with BMI 36.7, the differences in SAFs and S-values for the spine are 21.5% and 49% respectively. The highest differences in S-values are observed for the ribs (73.8%) and bladder (-64.4%). In XCAT phantom with BMI 35.53 the difference in SAFs and S-values for the spine is 23.8% and 47.4% respectively. The highest difference in S-value is observed in the ribs (79.6%). The difference in the S-value of bladder (-16.9%) is the smallest amongst the 3 BMIs that we tested.

Table 1: The SAF and S-value in different organs 18 hours after administration of 150mCi ^{153}Sm; comparison between dosimetry based on CT and XCAT phantom with BMI of 38.8. The source of activity is the SPECT.

Organs	SAF(1/kg)		Difference (%)	S-Value (mGy/MBq.S)		Difference (%)
	CT	XCAT with BMI38.8		CT	XCAT with BMI38.8	
Lung	0.0130	0.0114	12.3	7.11e-06	7.3915e-06	-3.90
Liver	0.0123	0.0089	27.6	2.90e-06	1.9503e-06	32.7
Kidney	0.0153	0.0123	19.6	1.94e-06	1.3962e-06	28.0
Spleen	0.0103	0.0117	-13.5	1.43e-06	1.2816e-06	10.4
Spine	0.0566	0.0414	26.8	1.83e-05	8.4580e-06	53.8
Rib Bone	0.0316	0.0265	16.1	4.68e-06	1.3706e-06	70.7
Bladder	0.0145	0.0103	28.9	1.64e-06	3.4215e-06	-109
Heart	0.0101	0.0087	13.8	1.09e-06	1.3788e-06	-26.5
Whole Body	0.0086	0.0081	5.8	2.0646e-06	2.0842e-06	-0.9

Table 2: The SAF and S-value in different organs 18 hours after administration of 150mCi ^{153}Sm; comparison between CT and XCAT with BMI 36.7 and 35.5 calculation. The source of activity is the SPECT.

Organs	SAF(1/kg)				S-Value (mGy/MBq.S)			
	XCAT with BMI36.7	Difference (%)	XCAT with BMI35.5	Difference (%)	XCAT with BMI36.7	Difference (%)	XCAT with BMI35.5	Difference (%)
Lung	0.0115	11.5	0.0093	28.4	6.7758e-06	4.7	6.0205e-06	15.3
Liver	0.0087	29.2	0.0090	26.8	1.9718e-06	32	2.2090e-06	23.8
Kidney	0.0106	30.7	0.0119	22.2	1.1123e-06	42.7	1.6672e-06	14.1
Spleen	0.0100	2.9	0.0099	3.8	1.3982e-06	2.2	1.3855e-06	3.1
Spine	0.0444	21.5	0.0431	23.8	9.3374e-06	49	9.6234e-06	47.4
Rib Bone	0.0264	16.4	0.0193	38.9	1.2278e-06	73.8	9.5588e-07	79.6
Bladder	0.0116	20	0.0121	16.5	2.6963e-06	-64.4	1.9177e-06	-16.9
Heart	0.0087	13.8	0.0088	12.8	1.7246e-06	-58.2	1.9161e-06	-75.8
Whole Body	0.0086	0	0.0084	2.3	2.3717e-06	-14.8	2.1852e-06	-5.8

The differences between the calculations based on CT and XCAT phantoms for all BMIs in kidney, liver, heart, spleen, bladder, lung, ribs and spine are considerable (Figures 2 & 3). As illustrated in the figures, the radiation to the spine is considerably higher when the CT data is used compared to XCAT; nevertheless, the whole body dosimetry results and the dosimetry of the lungs, liver, spleen and kidneys are rather the same between the calculations based on the CT data and the XCAT with different BMIs.

DISCUSSION

We observed similar whole body dosimetry results based on XCAT phantom with different BMIs and patient's CT data but remarkable differences between the dosimetry results for various organs (Table 1). These differences are higher than the acceptable variation of dosimetry results for clinical use [23]. The differences did not increase when unmatched BMI XCAT phantoms were used (Figures 2 & 3) which indicates that factors other than solely BMI are important in these calculations. Considering patient-specific dosimetry as the most available accurate method, our results show calculations on BMI matched XCAT phantom has remarkable differences from the CT based dosimetry. Hence, the whole body dosimetry is valid when calculations are done based on XCAT data instead of patient's CT, but the S-value and the SAF to the target organs may not be used interchangeably.

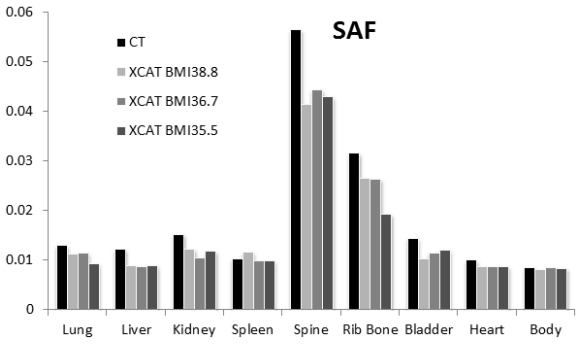

Fig 2. Comparison between SAFs of CT and XCAT phantom with different BMIs.

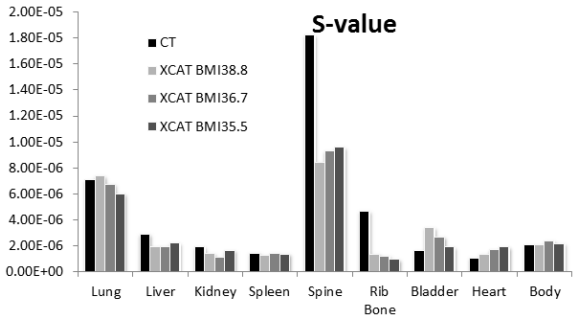

Fig 3. Comparison between S-values of CT and XCAT phantom with different BMIs.

The differences in the dosimetry results using the patient's individual CT and XCAT phantom were substantial in all employed BMIs. Similarity between the BMI used for XCAT design and patient did not decrease the extent of the error. Shape and size of the organs and the body composition may play a significant role in this regard. Given that the phantoms are based on the body composition of an individual subject, extrapolation to all patients is questionable. The differences in S-values infer that the patient's CT data cannot be safely substituted by XCAT phantom for calculation of the radiation of beta particle which exerts the therapeutic effect of the systemic radiations therapy [24]. The radiation to the spine and ribs could be underestimated when the XCAT data is employed (Figures 2 & 3). Also the absorbed doses in the lung and liver are underestimated with a lesser extent. The underestimation of the dose to the favorable target organs may cause overtreatment and increased risk of unfavorable side effects.

The similarity of the whole body dosimetry shows that the phantom and the calculation/simulations are generally acceptable. Variation between the organ boundaries and geometry of organs between patient and phantom may cause the differences and affect the organ dosimetry. On the other hand the quality of the segmentation of the organs in the CT image may contribute to finding; if the organs are not perfectly chosen the dosimetry would not be the real dosimetry for the organ.

In this study we used the GATE Monte Carlo code for calculation of absorbed dose. GATE code is already validated for dosimetry in many clinical situations including brachytherapy, external beam radiotherapy with photons/electrons, systemic radiotherapy, and proton-therapy. One of the main privileges of GATE is the capability to support both imaging and therapy modeling procedures [25]. The method we used has been employed with variations in other studies [26] for example to study mathematical phantom derived from the MIRD-type adult phantom.

The use of phantoms is already validated for internal dosimetry purposes [15, 20]. We previously reported that the dosimetry based on XCAT phantom is different from those based on the Zubal phantom [27] as well as different dosimetry estimations obtained from different XCAT BMIs [28, 29]. We showed that the differences corresponded to the different organ sizes. Hence, the different organ sizes between the patient and the phantom may affect the dosimetry and describes at least a part of denoted differences in the current study.

CONCLUSION

In this study, we showed that the results of dosimetry vary when the XCAT phantom is used in place of patient's CT image and the extent of the differences varies among XCAT phantoms with different BMIs. It seems that for treatment planning either we still need more accurate patient-specific dosimetry with patient own CT data, or humanoid phantoms need more adaptation to patient's characteristics.

Acknowledgment

We cordially thank Dr. Nahid Yaghoobi for her kind support with SPECT/CT acquisition and Dr. Paul Segars, the XCAT phantom developer, for his generous support for the XCAT data.

REFERENCES

1. Grimes J, Celler A, Birkenfeld B, Shcherbinin S, Listewnik MH, Piwowarska-Bilska H, Mikolajczak R, Zorga P. Patient-specific radiation dosimetry of 99mTc-HYNIC-Tyr3-octreotide in neuroendocrine tumors. J Nucl Med. 2011 Sep;52(9):1474-81.
2. Kolbert KS, Sgouros G, Scott AM, Bronstein JE, Malane RA, Zhang J, Kalaigian H, McNamara S, Schwartz L, Larson SM. Implementation and evaluation of patient-specific three-dimensional internal dosimetry. J Nucl Med. 1997 Feb;38(2):301-8.
3. Saeedzadeh E, Sarkar S, Abbaspour Tehrani-Fard A, Ay MR, Khosravi HR, Loudos G. 3D calculation of absorbed dose for 131I-targeted radiotherapy: a Monte Carlo study. Radiat Prot Dosimetry. 2012 Jul;150(3):298-305.

4. Sgouros G, Kolbert KS, Sheikh A, Pentlow KS, Mun EF, Barth A, Robbins RJ, Larson SM. Patient-specific dosimetry for 131I thyroid cancer therapy using 124I PET and 3-dimensional-internal dosimetry (3D-ID) software. J Nucl Med. 2004 Aug;45(8):1366-72.

5. Tsougos I, Loudos G, Georgoulias P, Theodorou K, Kappas C. Patient-specific internal radionuclide dosimetry. Nucl Med Commun. 2010 Feb;31(2):97-106.

6. Dewaraja YK, Frey EC, Sgouros G, Brill AB, Roberson P, Zanzonico PB, Ljungberg M. MIRD pamphlet No. 23: quantitative SPECT for patient-specific 3-dimensional dosimetry in internal radionuclide therapy. J Nucl Med. 2012 Aug;53(8):1310-25.

7. Buck AK, Nekolla S, Ziegler S, Beer A, Krause BJ, Herrmann K, Scheidhauer K, Wester HJ, Rummeny EJ, Schwaiger M, Drzezga A. SPECT/CT. J Nucl Med. 2008 Aug;49(8):1305-19.

8. Dewaraja YK, Wilderman SJ, Koral KF, Kaminski MS, Avram AM. Use of integrated SPECT/CT imaging for tumor dosimetry in I-131 radioimmunotherapy: a pilot patient study. Cancer Biother Radiopharm. 2009 Aug;24(4):417-26.

9. Segars WP, Sturgeon G, Mendonca S, Grimes J, Tsui BMW. 4D XCAT phantom for multimodality imaging research. Med Phys. 2010 Sep;37(9):4902-15.

10. Bauman G, Charette M, Reid R, Sathya J. Radiopharmaceuticals for the palliation of painful bone metastasis-a systemic review. Radiother Oncol. 2005 Jun;75(3):258-70.

11. Jan S, Santin G, Strul D, Staelens S, Assié K, Autret D, Avner S, Barbier R, Bardiès M, Bloomfield PM, Brasse D, Breton V, Bruyndonckx P, Buvat I, Chatziioannou AF, Choi Y, Chung YH, Comtat C, Donnarieix D, Ferrer L, Glick SJ, Groiselle CJ, Guez D, Honore PF, Kerhoas-Cavata S, Kirov AS, Kohli V, Koole M, Krieguer M, van der Laan DJ, Lamare F, Largeron G, Lartizien C, Lazaro D, Maas MC, Maigne L, Mayet F, Melot F, Merheb C, Pennacchio E, Perez J, Pietrzyk U, Rannou FR, Rey M, Schaart DR, Schmidtlein CR, Simon L, Song TY, Vieira JM, Visvikis D, Van de Walle R, Wieërs E, Morel C. GATE: a simulation toolkit for PET and SPECT. Phys Med Biol. 2004 Oct 7;49(19):4543-61.

12. Strulab D, Santin G, Lazaro D, Breton V, Morel C. GATE (geant4 application for tomographic emission): a PET/SPECT general-purpose simulation platform. Nucl Phys B Proc Suppl. 2003;125:75-79.

13. Jan S, Benoit D, Becheva E, Carlier T, Cassol F, Descourt P, Frisson T, Grevillot L, Guigues L, Maigne L, Morel C, Perrot Y, Rehfeld N, Sarrut D, Schaart DR, Stute S, Pietrzyk U, Visvikis D, Zahra N, Buvat I. GATE V6: a major enhancement of the GATE simulation platform enabling modelling of CT and radiotherapy. Phys Med Biol. 2011 Feb 21;56(4):881-901.

14. Taschereau R, Chow PL, Cho JS, Chatziioannou AF. A microCT X-ray head model for spectra generation with Monte Carlo simulations. Nucl Instrum Methods Phys Res A. 2006;569(2):373-377.

15. Parach AA, Rajabi H. A comparison between GATE4 results and MCNP4B published data for internal radiation dosimetry. Nuklearmedizin. 2011;50(3):122-133.

16. Visvikis D, Bardies M, Chiavassa S, Danford C, Kirov A, Lamare F, Maigne L, Staelens S, Taschereau R. Use of the GATE Monte Carlo package for dosimetry applications. Nucl Instrum Methods Phys Res A. 2006;569(2):335-340.

17. Agostinelli S, Allison J, Amako K, Apostolakis J, Araujo H, Arce P, Asai M, Axen D, Banerjee S, Barrand G, Behner F, Bellagamba L, Boudreau J, Broglia L, Brunengo A, Burkhardt H, Chauvie S, Chuma J, Zschiesche D. GEANT4—a simulation toolkit. Nucl Instrum Methods Phys Res A. 2003;506(3):250-303.

18. Song Y, Luboz V, Din N, King D, Gould D, Bello F, Bulpitt A. Segmentation of 3D vasculatures for interventional radiology simulation. Stud Health Technol Inform. 2011;163:599-605.

19. Fallahpoor M, Abbasi M, Sen A, Parach A, Kalantari F. SU-C-201-06: Utility of Quantitative 3D SPECT/CT Imaging in Patient Specific Internal Dosimetry of 153-Samarium with GATE Monte Carlo Package. Med Phys. 2015;42(6):3203.

20. Parach AA, Rajabi H, Askari MA. Paired organs-should they be treated jointly or separately in internal dosimetry? Med Phys. 2011 Oct;38(10):5509-21.

21. Loevinger R, Budinger TF, Watson EE. MIRD primer for absorbed dose calculations. New York: Society of Nuclear Medicine; 1988.

22. Bolch WE, Eckerman KF, Sgouros G, Thomas SR. MIRD pamphlet No. 21: a generalized schema for radiopharmaceutical dosimetry--standardization of nomenclature. J Nucl Med. 2009 Mar;50(3):477-84.

23. American Association of Physicists in Medicine. Physical aspects of quality assurance in radiation therapy. New York: American Institute of Physics; 1994.

24. O'Donoghue JA, Bardiès M, Wheldon TE. Relationships between tumor size and curability for uniformly targeted therapy with beta-emitting radionuclides. J Nucl Med. 1995 Oct;36(10):1902-9.

25. Sarrut D, Bardiès M, Boussion N, Freud N, Jan S, Létang JM, Loudos G, Maigne L, Marcatili S, Mauxion T, Papadimitroulas P, Perrot Y, Pietrzyk U, Robert C, Schaart DR, Visvikis D, Buvat I. A review of the use and potential of the GATE Monte Carlo simulation code for radiation therapy and dosimetry applications. Med Phys. 2014 Jun;41(6):064301.

26. Díaz-Londoño G, García-Pareja S, Salvat F, Lallena AM. Monte Carlo calculation of specific absorbed fractions: variance reduction techniques. Phys Med Biol. 2015 Apr 7;60(7):2625-44.

27. Fallahpoor M, Abbasi M, Kalantari F, Parach AA, Sen A. Practical Nuclear Medicine and Utility of Phantoms for Internal Dosimetry: XCAT Compared with Zubal. Radiat Prot Dosimetry. 2017 Apr 25;174(2):191-197.

28. Fallahpoor M, Abbasi M, Parach AA, Kalantari F. Internal dosimetry for radioembolization therapy with Yttrium-90 microspheres. J Appl Clin Med Phys. 2017 Mar;18(2):176-180.

29. Fallahpoor M, Abbasi M, Parach AA, Kalantari F. The importance of BMI in dosimetry of 153Sm-EDTMP bone pain palliation therapy: A Monte Carlo study. Appl Radiat Isot. 2017 Jun;124:1-6.